

BROKEN SYMMETRY OF RECRUITMENT FLUCTUATIONS IN MARINE FISHES: LÉVY-STABLE LAWS AND BEYOND

H.-S. NIWA

ABSTRACT. Recruitment is calculated by summing random offspring-numbers entering the population, where the number of summands (i.e. spawning population size) is also a random process. A priori, it is not clear that individual reproductive variability would have a significant impact on aggregate measures for monitoring populations. Usually these variations are averaged out in a large population, and the aggregate output is merely influenced by population-wide environmental disturbances such as climate and fisheries. However, such arguments break down if the distribution of the individual offspring numbers is heavy-tailed. In a world with power-law offspring-number distribution with exponent $1 < \alpha < 2$, the recruitment distribution has a putative power-law regime in the tail with the same α . The question is to what extent individual reproductive variability can have a noticeable impact on the recruitment under environmentally driven population fluctuations. This question is answered by considering the Lévy-stable fluctuations as embedded in a randomly varying environment. I report fluctuation scaling and asymmetric fluctuations in recruitment of commercially exploited fish stocks throughout the North Atlantic. The linear scaling of recruitment standard deviation with recruitment level implies that the individual reproductive variability is dominated by population fluctuations. The totally asymmetric (skewed to the right) character is a sign of idiosyncratic variation in reproductive success.

1. INTRODUCTION

Marine populations of mass-spawning species are characterized by intermittent, large recruitment events (Hjort 1914). Very large interfamilial, or idiosyncratic, variation in reproductive success has been documented in marine species (Hedgecock & Pudovkin 2011). Population models with skewed offspring-number distributions have recently been proposed as appropriate models to investigate gene genealogies for abundant marine species with type-III (exponential) survivorship curves (Eldon & Wakeley 2006, Sargsyan & Wakeley 2008). Patterns of genetic variation have been studied to search for the imprint of multiple mergers of ancestral lineages (Steinrücken et al. 2013, Eldon et al. 2015, Árnason & Halldórsdóttir 2015). The ‘imprint’ is a sign of the domination by a single or a few families in the population. Niwa et al. (2016) showed that the multiple-merger coalescent model of the Beta($2 - \alpha, \alpha$) type provides a better fit of Japanese sardine genetic variation than Kingman’s (1982) classical coalescent model. The Beta($2 - \alpha, \alpha$) coalescent arises from a population model with power-law offspring-number distribution with exponent $1 < \alpha < 2$ (Schweinsberg 2003). While the recruiting process has exponential decay in survival probability, the exponential amplification of the number

Key words and phrases. random sums; idiosyncratic reproductive variation; α -stable law; Taylor’s law; Gibrat’s law; North Atlantic fishes.

of successfully recruiting offspring (littermates or siblings) in a family compensates the exponentially small probability of their surviving to reproductive maturity. The combination of these two exponentials leads to power laws in the offspring-number distribution (Reed & Hughes 2002, Newman 2005, Niwa et al. 2017).

Recruitment is calculated by summing random offspring numbers, where the number of summands (i.e. spawning population size) is also a random process. Under the power-law model of offspring-number distribution, the exponent α being less than two qualifies the recruitment distribution as belonging to the Lévy-stable distribution regime (Lévy 1925, Khintchine & Lévy 1936, Lévy 1937), so that the tail of the recruitment distribution follows a power law with the same exponent α and thus, the recruitment distribution has diverging second moment (infinite variation). One also expects that the distribution of relative changes in recruitment (i.e. recruitment growth-rates) over a one-year interval is symmetric and Lévy-stable with the same exponent α .

On the other hand, the match-mismatch hypothesis (Cushing 1990) has been used to describe climate effects on the interannual variability in marine fish recruitment and thus, recruitment is primarily regulated by abiotic (i.e. density-independent) factors. If individual reproductive outputs (or family sizes) have a small dispersion (relative to year-to-year variation in population sizes, or in carrying capacity of environment), the reproductive variations in birth and death process lead to negligible aggregate fluctuations in a large population. Consequently, environmentally driven fluctuations in (spawning) population sizes appear to explain macroscopic (aggregate) fluctuations. So that individual reproductive variations cannot be extracted from population-level measurements (e.g. interannual recruitment variability).

I show that, in spite of strong fluctuations in the population size (carrying capacity), the above argument on the (negligible) aggregate effect breaks down if the distribution of family sizes is heavy-tailed. This paper discusses how, in a world with power-law offspring-number distribution (with exponent $1 < \alpha < 2$), idiosyncratic individual-level fluctuations (i.e. differences in individual reproductive successes, or variances of family sizes) aggregate up to non-trivial aggregate fluctuations in a large population under a randomly varying environment. The idiosyncratic reproductive variability is quantitatively large enough to matter at the population level. In this instance, the distribution of recruitment growth-rates is not symmetric, but is instead totally asymmetric (skewed to the right) and heavy-tailed with the same exponent α . I contend that aggregate fluctuations come in tail part from idiosyncratic reproductive behavior, even though the fluctuations of the sums of individual reproductive outputs are dominated by population-wide factors such as climate and fisheries. Of particular interest is to what extent the idiosyncratic reproductive variations are averaged out upon aggregation under population fluctuations.

The paper is organized as follows. Section 2 introduces a recruitment model. Section 3 reports some stylized facts regarding recruitment variations in commercially exploited fish stocks. Section 4 presents model calculations in a stable-distribution framework based on random sums of random variables, which connect all those observations. Then, Section 5 numerically deals with nonvanishing aggregate fluctuations. Finally, Section 6 concludes.

2. RECRUITMENT MODEL

The (spawning) population size is the number of reproductively-successful individuals in a generation. Their offspring numbers are independent copies of random variable X with asymptotic probability distribution

$$\Pr(X \geq x) \simeq (x_0/x)^\alpha, \quad (1)$$

which, with $1 < \alpha < 2$ and $x_0 > 0$, decays slowly as $x \rightarrow \infty$. The offspring-number distribution has finite mean (assumed greater than one) and infinite variance. Define N_t , the size of the population at time t , to be random variables with finite mean $\langle N \rangle$. Angled brackets denote mean over all possible realizations. The recruitment is the total number of offspring entering the (potentially reproductive) population. Let R_t denote the number of recruits to the population at time $t + 1$ in years (or generations),

$$R_t = \sum_{n=1}^{N_t} X_n,$$

where X_n is the number of offspring of the n -th individual in year t with the distribution in Equation (1) being identical for all t (i.e. the number of summands is independent of the summands X_n). The offspring generation is constituted by sampling N_{t+1} out of R_t potential offspring. The average recruitment is given by

$$\langle R \rangle = \langle X \rangle \langle N \rangle$$

with mean offspring number $\langle X \rangle > 1$. The amplitude of fluctuations in N_t is given by

$$\Sigma_N^2 = \frac{\sum_{t=1}^T (N_t - \langle N \rangle)^2}{T},$$

where T is the number of trials (generations) of a random process. The amplitude of fluctuations in R_t is given by

$$\Sigma_R^2 = \frac{\sum_{t=1}^T (R_t - \langle R \rangle)^2}{T}.$$

Temporal variation is considered by examining the relative (or absolute) variation of the recruitment, instead of the change in the logarithm of the recruitment. Let η_t be the relative change (i.e. the percentage growth rate) in recruitment over a year,

$$\eta_t = \frac{R_{t+1} - R_t}{R_t},$$

where $R_{t+1} - R_t$ is the increment (absolute difference) of recruitment between two successive years (or generations). It is assumed that $\langle \eta \rangle = 0$ and $\langle R_{t+1} - R_t \rangle = 0$. The amplitude of fluctuations in η_t is given by

$$\Sigma_\eta^2 = \frac{\sum_{t=1}^{T-1} \eta_t^2}{T-1}.$$

When there are several stocks (subsystems with respect to the habitat of the species) for which one observes year-class recruitment, the difference between stocks with smaller and greater mean recruitment comes from the different mean number of spawners. One is interested in how the sample standard deviation changes, across stocks, with the value of the mean annual recruitment to individual stocks. One then calculates the $\langle R^i \rangle$ and Σ_{R^i} (where the superscript i denotes the stock

identifier), and compares the couplings across stocks to investigate whether stocks with larger mean recruitment exhibit larger fluctuations. The relationship will be extracted as

$$\Sigma_{R^i} \propto \langle R^i \rangle^b \quad (2)$$

with scaling exponent b being constant (and with the same prefactor) for all stocks. This type of scaling relationship is called (a kind of) Taylor’s (1961) law or fluctuation scaling (Eisler et al. 2008). The scaling law states that the fluctuations (the sample standard deviation of each stock) can be represented by a power-law function of the corresponding average. The scaling exponent b is usually between 1/2 and 1 (Eisler et al. 2008). Then, the standard deviation in recruitment growth-rate η^i should decay as the $(b - 1)$ power of average recruitment,

$$\Sigma_{\eta^i} \propto \langle R^i \rangle^{b-1}. \quad (3)$$

Model calculations employ a stable-distribution formalism based on random sums of random variables. In this context the emergence of fluctuation scaling is equivalent to some corresponding limit theorems.

3. STATISTICAL ANALYSIS

This section provides insight in understanding the empirical properties of fish recruitment variability.

3.1. Data. Time-series data (same as Niwa 2022a) were taken from International Council for the Exploration of the Sea, archived at <http://www.ices.dk/advice/Pages/Latest-Advice.aspx>. There were 72 fish stocks analyzed throughout the North Atlantic: 19 pelagic stocks (7 species: capelin, herring, horse mackerel, mackerel, sardine, sprat and blue whiting), 50 demersal stocks (16 species: white anglerfish, cod, haddock, hake, Greenland halibut, megrim, four-spot megrim, plaice, Norway pout, beaked redfish, golden redfish, saithe, sandeel, seabass, sole and whiting), 2 deep-water stocks (2 species: ling and tusk) and one crustacean stock (northern shrimp). The lengths of these time-series varied from 18 to 72 years.

3.2. Empirical results. Figure 1a shows that the recruitment data (in thousand fish, upper solid gray circles) across 72 stocks (regardless of species) collapse onto the upper solid line $\Sigma_R \propto \bar{R}$ with prefactor

$$\left[\overline{\Sigma_{R^i}^2 / \bar{R}^{i^2}} \right]^{1/2} = 0.766$$

(average across stocks) over five orders of magnitude in \bar{R} , where the overbar denotes sample mean. The spawning biomass data (in tonnes, upper open circles) also exhibit linear scaling $\Sigma_N \propto \bar{N}$ with prefactor

$$\left[\overline{\Sigma_{N^i}^2 / \bar{N}^{i^2}} \right]^{1/2} = 0.522$$

(dashed line).

Figure 1a also shows that the sample standard deviation of relative changes in recruitment (lower solid black circles) hovers around $y = 1$ (lower solid line), independent of \bar{R}^i . The lower open circles plot the sample standard deviation of relative changes in spawning-stock biomass versus average abundance.

I now study the absolute differences between two consecutive values in recruitment series, where the time series is detrended by subtracting the mean trend. The

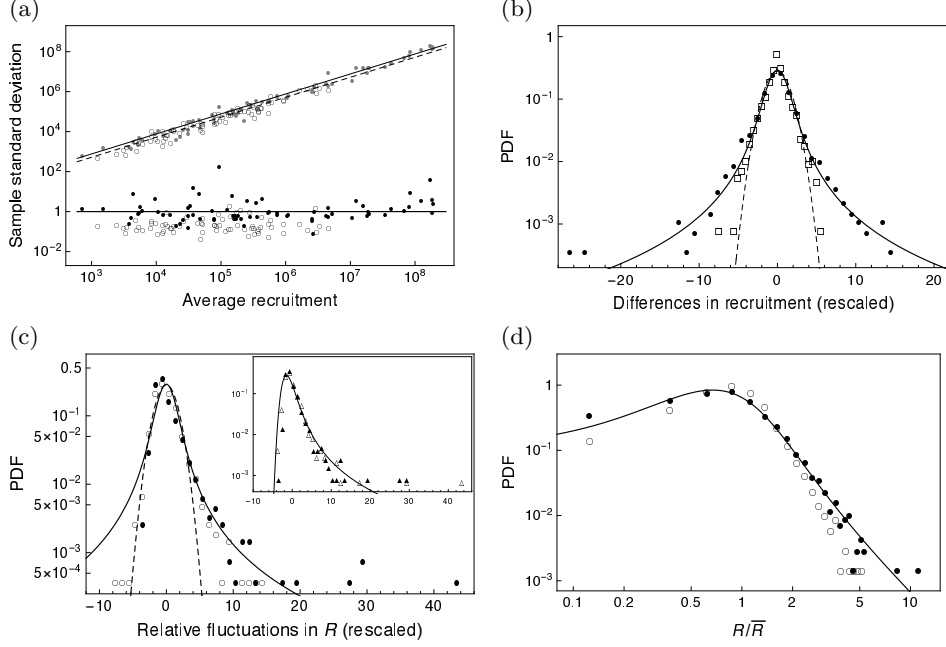


FIG. 1. Statistical analysis of stock-recruitment data from the North Atlantic. (a) Fluctuation scaling for Σ_R (upper solid gray circles) and Σ_η (lower solid circles) among stocks (R^i in units of 10^3). (b) Leptokurtic distribution of successive differences in recruitment. (c) Asymmetric distributions of relative changes in recruitment (solid circles). In the inset, open (resp. solid) triangles are plotted for autocorrelated (resp. non-autocorrelated) series of recruitment data. (d) Distributions of normalized recruitment (solid circles). In these panels, open circles are for the spawning-stock biomass (in tonnes).

successive differences are rescaled with the fluctuation width (i.e. scale factor) by stocks, where the scale factor is estimated by the root-median-square successive differences of the (detrended) recruitment series (Takayasu et al. 2014). The rescaled distributions with zero mean and unity width, when aggregated across 72 stocks, fit a symmetric Lévy-stable distribution with exponent $\hat{\alpha} = 1.42$ (maximum likelihood estimate); see Figure 1b (solid circles with solid line). Further, using the standard deviation divided by $\sqrt{2}$, when the absolute differences of recruitment are rescaled by stock and aggregated across stocks, the shape of the distribution (open squares in Figure 1b) is more concentrated than the Gaussian distribution (with mean zero and standard deviation $\sqrt{2}$, dashed line), and the tails are heavier than it.

Figure 1c shows that the relative changes in recruitment, when aggregated across 72 stocks, follow closely the maximally asymmetric Lévy-stable distribution with exponent $\hat{\alpha}$ (with the tail vanishing to the left), where the data are rescaled with their root-median-square values by stock, after detrended by subtracting the mean trend. The solid line in the main panel is the symmetric Lévy-stable distribution with exponent $\hat{\alpha}$ (and with zero mean and unity width), and the dashed line is the Gaussian distribution with mean zero and standard deviation $\sqrt{2}$. The relative

changes in spawning-stock biomass, rescaled with their root-median-square values by stock (after detrended by subtracting the mean trend), also exhibit totally skewed or asymmetric character (open circles, with data aggregated across stocks), which is close to the rescaled distribution of recruitment growth-rates. Temporal autocorrelation may act to increase or decrease the fluctuation width of growth rates. Figure 1c (inset) shows that for 36 (solid triangles) out of 72 recruitment series that have passed the Ljung-Box test at the 5% level, which reasonably satisfy the assumption of no autocorrelation, the recruitment growth-rates collapse onto those for the rest (open triangles) of the recruitment series showing some evidences of autocorrelation, where data are aggregated across stocks after rescaled by the fluctuation width. The solid line in the inset is the maximally asymmetric Lévy-stable distribution with exponent $\hat{\alpha}$ (with zero mean and unity width).

Figure 1d shows that the normalized recruitment data R_t^i/\bar{R}^i (solid circles, aggregated across stocks) collapse upon a universal curve (scaling function). I verify the fitting of a Lévy-stable distribution (solid line). Under the stable law with $\hat{\alpha} = 1.42$, the degree of asymmetry is estimated at one by maximum likelihood, and the maximum likelihood estimate of location (resp. scale) is 1.16 (resp. 0.332). Furthermore, the distribution of the normalized variables R_t^i/\bar{R}^i is close to that for the N_t^i/\bar{N}^i (open circles) in the central part.

3.3. Stylized facts on recruitment fluctuations. Analyzing fisheries stock-recruitment data from the North Atlantic, I have found the following results: (i) the linear dependence of the amplitude of recruitment fluctuations on recruitment level, (ii) the independence of the variation in relative recruitment changes from recruitment level, (iii) the leptokurtic character of (absolute) recruitment increments, and (iv) the totally asymmetric character of the distribution of relative recruitment changes.

The linear scaling of fluctuations in abundance of populations was reported for the North Sea fish community (Cobain et al. 2019). In this paper, I have found that the per-recruit variability in recruitment is close to the per-capita variability in population abundance, and both of these are constant for all stocks. The scaling exponent of $b = 1$ as in Equation (2) indicates that the recruitment series R_t^i 's are rescaled with \bar{R}^i (times a constant), and the normalized observations have a universal distribution. The scaling function is very close to a maximally asymmetric Lévy-stable distribution.

The asymmetric (skewed to the right) character of the distribution of relative changes has been repeatedly observed in a variety of animal (insect, bird, mammal and fish) populations (Keitt & Stanley 1998, Allen et al. 2001, Keitt et al. 2002, Niwa 2006, 2007, Lan & Chandran 2011). Another, much less studied property is the scaling relationship between the standard deviation and average of the growth-rate distribution (Keitt et al. 2002, Niwa 2006). In this paper, I have found that the amplitude of fluctuations in recruitment growth-rate η is approximately independent of the recruitment level, which is a version of Gibrat's (1931) law for variances. The amplitude of fluctuations in year-to-year percentage population growth-rate is also approximately independent of population size.

A conventional approach uses the log-normal distribution of fish recruitment (Hilborn & Walters 1992). The ratio of two numbers, each drawn from a log-normal distribution, is also log-normally distributed, so the distribution of $R_{t+1}/R_t (= \eta_t + 1)$ would be log-normal as well. Further, the difference of two log-normal

random variables should resemble a Gaussian distribution (Carmona & Durrelman 2003). I have found that the distribution of (absolute) recruitment increments is not Gaussian but rather leptokurtic. The representation of recruitment increments as symmetric Lévy-stable random variables may account for their leptokurtic character. However, it has a drawback: the relative fluctuations in recruitment have totally skewed properties, showing in fact they appear to be a maximally asymmetric Lévy-stable distribution. These apparently contradictory aspects will be blended together into a consistent picture in the following section. A statistical test for log-normality of the data is provided in Niwa (2022a).

4. MODEL CALCULATIONS

4.1. Lévy-stable fluctuations. Consider the sum of N independent random variables X_1, \dots, X_N with a power-law distribution in Equation (1) of exponent α in (1, 2). If the population size N is fixed constant in an environment with constant carrying capacity, the sum $R = \sum_{n=1}^N X_n$ has a mean $\langle R \rangle = \langle X \rangle N$, and as $N \rightarrow \infty$, the rescaled sum $(R - \langle R \rangle)/N^{1/\alpha}$ has a limit distribution, i.e. a maximally asymmetric Lévy-stable law of exponent α . The tail vanishes to the left, and the assumption $\langle X \rangle > 1$ ensures that $R > N$ with sufficiently high probability. Since X_n^2 follows a power-law distribution with exponent $\alpha/2 < 1$, one has, as $N \rightarrow \infty$,

$$(R - \langle R \rangle)^2 \approx \sum_{n=1}^N (X_n - \langle X \rangle)^2 \simeq x_0^2 C_{\alpha/2} N^{2/\alpha} w$$

with $C_{\alpha/2} = [\Gamma(1 - \alpha/2) \cos(\pi\alpha/4)]^{2/\alpha}$, where w is a random variable with maximally asymmetric Lévy-stable distribution with exponent $\alpha/2$ and width (scale factor) of unity (Gabaix 2011). The distribution of w does not depend on N . The recruitment growth-rate follows

$$\eta^2 \simeq 2^{2/\alpha} (x_0 / \langle X \rangle)^2 C_{\alpha/2} N^{2(1/\alpha - 1)} w.$$

Accordingly, the recruitment variability scales as

$$\Sigma_R \propto \langle R \rangle^{1/\alpha} T^{1/\alpha - 1/2} \quad (4)$$

$$\Sigma_\eta \propto \langle R \rangle^{1/\alpha - 1} T^{1/\alpha - 1/2} \quad (5)$$

with exponent $b = 1/\alpha$ as in Equations (2) and (3), where $T (\gg 1)$ is the number of trials (Bouchaud & Georges 1990, Newman 2005). Note that the variances $\langle (R - \langle R \rangle)^2 \rangle$ and $\langle \eta^2 \rangle$ are infinite.

Define $X_{1,N} \geq X_{2,N} \geq \dots \geq X_{N,N}$ by ranking in decreasing order the values encountered among the N terms of the sum R . When $1 < \alpha < 2$, one has, for large N ,

$$\begin{aligned} \langle X_{1,N} \rangle &= \frac{x_0 N! \Gamma(1 - 1/\alpha)}{\Gamma(N + 1 - 1/\alpha)} \approx x_0 \Gamma(1 - 1/\alpha) N^{1/\alpha} \\ \langle X_{2,N} \rangle &= \frac{\alpha - 1}{\alpha} \langle X_{1,N} \rangle \end{aligned}$$

and while $X_{1,N}$ has an infinite second moment (infinite variation), one has

$$\begin{aligned}\langle X_{2,N}^2 \rangle &= \frac{x_0^2 N! \Gamma(2 - 2/\alpha)}{\Gamma(N + 1 - 2/\alpha)} \approx x_0^2 \Gamma(2 - 2/\alpha) N^{2/\alpha} \\ \langle X_{1,N} X_{2,N} \rangle &= \frac{\alpha}{\alpha - 1} \langle X_{2,N}^2 \rangle\end{aligned}$$

(Zaliapin et al. 2005), where the Euler product formula for the gamma function is used. Importantly, all but the largest order statistics have finite second moment. Therefore, the sum $R_{2,N} (= \sum_{k=2}^N X_{k,N})$ of the $(N - 1)$ lower order statistics converges to a Gaussian-distributed random variable with first two moments given by

$$\langle R_{2,N} \rangle \approx \frac{x_0 \alpha}{\alpha - 1} (N - \Gamma(2 - 1/\alpha) N^{1/\alpha}) \approx \langle R \rangle$$

and

$$\langle R_{2,N}^2 \rangle = \left\langle \sum_{k=2}^N X_{k,N}^2 \right\rangle + \left\langle \sum_{k \neq \ell} X_{k,N} X_{\ell,N} \right\rangle \sim N^{2/\alpha},$$

where

$$\left\langle \sum_{k=2}^N X_{k,N}^2 \right\rangle \approx \frac{x_0^2 \alpha}{\alpha - 2} (N - \Gamma(2 - 2/\alpha) N^{2/\alpha}) \approx \frac{\alpha}{2 - \alpha} \langle X_{2,N}^2 \rangle,$$

and where

$$\begin{aligned}\langle X_{2,N} X_{3,N} \rangle &= \frac{2\alpha}{2\alpha - 1} \langle X_{3,N}^2 \rangle \\ \langle X_{2,N} X_{4,N} \rangle &= \frac{3! \alpha^2}{(2\alpha - 1)(3\alpha - 1)} \langle X_{4,N}^2 \rangle\end{aligned}$$

etc. Accordingly, while the sum R is dominated by its largest term $X_{1,N}$, the sample-to-sample variations in recruitment (Σ_R) and in growth rates (Σ_η) are sensitive to central observations in the vast majority and insensitive to the rare tail events.

The recruitment R follows a power-law distribution with exponent α in the tail

$$R - \langle R \rangle \gtrsim N^{1/\alpha},$$

i.e. $R \gtrsim \langle X \rangle N$ for large N , so the fraction of the total recruits, $(R - \langle R \rangle) / \langle R \rangle \sim N^{1/\alpha - 1}$, can be linked to one parent. The recruitment growth-rates are symmetrically and Lévy-stable distributed, and follow a power law asymptotically with exponent α in the tails

$$|\eta| \gtrsim N^{1/\alpha - 1},$$

because the size of the largest family $X_{1,N}$ scales as $N^{1/\alpha}$.

4.2. Beyond the Lévy-stable fluctuations. To incorporate externally induced fluctuations, let us allow N to vary independently from one year to the other. The R_t 's are independent. Recruitment variability contains contributions as a result of individual reproductive variations and population-size (or carrying-capacity) fluctuations, both of which are sources of fluctuations in output productivity. It then follows that

$$(R_t - \langle R \rangle)^2 = (R_t - \langle X \rangle N_t)^2 + \langle X \rangle^2 (N_t - \langle N \rangle)^2 + 2 \langle X \rangle (R_t - \langle X \rangle N_t) (N_t - \langle N \rangle),$$

yielding

$$\Sigma_R^2 \simeq x_0^2 C_{\alpha/2} \langle N \rangle^{2/\alpha} T^{2/\alpha-1} w + \langle X \rangle^2 \Sigma_N^2$$

for large $\sum_{t=1}^T N_t \approx \langle N \rangle T$. Assume $\Sigma_N / \langle N \rangle \ll 1$, so that $\Sigma_R / \langle R \rangle \ll 1$. Then, one has

$$\Sigma_\eta^2 \approx 2\Sigma_R^2 / \langle R \rangle^2.$$

When the amplitude of fluctuations Σ_N is typically less than $\langle N \rangle^{1/\alpha}$, i.e. the ratio $\Sigma_N / \langle N \rangle^{1/\alpha}$ approaches 0 as $\langle N \rangle$ gets large, one recovers Equations (4) and (5).

When the Σ_N exceeds the threshold, i.e. the ratio $\Sigma_N / \langle N \rangle^{1/\alpha}$ goes to infinity as $\langle N \rangle \rightarrow \infty$ with $\Sigma_N / \langle N \rangle$ kept finite ($\ll 1$), one typically has

$$\Sigma_R \approx \langle X \rangle \Sigma_N,$$

which leads to

$$\Sigma_R / \langle R \rangle \approx \Sigma_N / \langle N \rangle.$$

The typical relative change in recruitment over a year is then estimated by

$$\Sigma_\eta \approx \sqrt{2} \Sigma_N / \langle N \rangle. \quad (6)$$

Therefore, under environmentally driven population fluctuations with $\Sigma_N \propto \langle N \rangle$, the recruitment variability scales as

$$\begin{aligned} \Sigma_R &\propto \langle R \rangle \\ \Sigma_\eta &\sim 1 \end{aligned}$$

with exponent $b = 1$ as in Equations (2) and (3), where the prefactors in the scaling relations may depend on T through Σ_N .

A generic representation of the recruitment dynamics is given by

$$R_t = x_0 C_\alpha N_t^{1/\alpha} z_t + \langle X \rangle N_t \quad (7)$$

with z_t being distributed as the maximally asymmetric Lévy-stable law of exponent α with zero mean and unity width, where $C_\alpha = [\Gamma(1 - \alpha) \cos(\pi\alpha/2)]^{1/\alpha}$. The variable z_t is independent of N_t . If $\Sigma_N / \langle N \rangle^{1/\alpha} \rightarrow 0$ as $\langle N \rangle \rightarrow \infty$, one has

$$R_t \simeq x_0 C_\alpha \langle N \rangle^{1/\alpha} z_t + \langle X \rangle \langle N \rangle, \quad (8)$$

and consequently,

$$\eta_t \simeq x_0 C_\alpha \frac{z_{t+1} - z_t}{\langle X \rangle \langle N \rangle^{1-1/\alpha}},$$

which follows a symmetric Lévy-stable distribution with exponent α . If $\Sigma_N / \langle N \rangle^{1/\alpha} \rightarrow \infty$ as $\langle N \rangle \rightarrow \infty$, one has

$$R_t \simeq \langle X \rangle N_t, \quad (9)$$

and consequently,

$$\eta_t \simeq \frac{N_{t+1} - N_t}{N_t}.$$

As the Σ_N increases with increasing environmental disturbances, the fluctuation width of η_t broadens, asymptotically to give Equation (6). When

$$|\eta_t| \gtrsim \sqrt{2} \Sigma_N / \langle N \rangle \quad (10)$$

with scaling $\Sigma_N \propto \langle N \rangle$, idiosyncratic variations do not die out in the aggregate, and η_t 's follow a power-law distribution with the same exponent α as the offspring-number distribution. Therefore, the growth-rate distribution is maximally asymmetric for large $\langle N \rangle$, since the tail vanishes to the left. Besides the recruitment growth-rates, the recruitment distribution also has a putative power-law regime with exponent α in the tail

$$R_t - \langle R \rangle \gtrsim \Sigma_R, \quad (11)$$

i.e. $R_t \gtrsim \langle R \rangle$. So the outer tails still reflect the idiosyncratic reproductive fluctuations. Contrariwise, the recruitment movements mimic the population-size (carrying-capacity) fluctuations in the central regions

$$R_t \lesssim \langle R \rangle + \Sigma_R \quad (12)$$

$$|\eta_t| \lesssim \Sigma_\eta \quad (13)$$

where individual offspring-number fluctuations have a negligible aggregate effect in the limit of large $\langle N \rangle$. The right-hand sides of Equations (10–13) are evaluated in the limit of $T \rightarrow 1$, if the Σ_N depends on T .

Remark. When environmental stochasticity imposes strong fluctuations in N , if $\Sigma_N \propto \langle N \rangle$, the linear-scaling behavior, $\Sigma_R \propto \langle R \rangle$, emerges (see also Anderson et al. 1982, de Menezes & Barabási 2004, Niwa 2022a). If the per-capita variability in population abundance ($\Sigma_{N^i} / \langle N^i \rangle$) is constant across stocks, it is assumed that the normalized abundances, $\nu_t = N_t^i / \langle N^i \rangle$, are identically distributed across stocks (Eisler et al. 2008). If this is true, one has

$$\Sigma_{N^i} = \Sigma_\nu \langle N^i \rangle$$

with $\Sigma_\nu^2 = \overline{[\Sigma_{N^i}^2 / \langle N^i \rangle^2]}$ (average across stocks). Further, from Equation (9) as $N \rightarrow \infty$, the normalized recruitment $R_t^i / \langle R^i \rangle$ is equal (in distribution) to the universal random variable ν_t , which gives rise to a linear relationship

$$\Sigma_{R^i} \approx \Sigma_\nu \langle R^i \rangle. \quad (14)$$

Even though the tail exponents of the offspring distributions are stock-specific, Equation (14) holds. In this case, the normalized variables $R_t^i / \langle R^i \rangle$ are almost identically distributed on the central part across stocks.

5. SIMULATION

Consider the environmental (carrying-capacity) fluctuations as embedded in a confining well or barrier, ensuring mean-reverting behavior, without having to rely on details of regulation in the system. N_t individuals in year t are sampled (selected for reproduction) out of R_{t-1} extant individuals in year $t-1$. A random variable N_t is drawn according to a truncated (maximally asymmetric) Lévy-stable distribution bounded below at R_{t-1} , where the distribution has a scale factor ς_N and a location parameter $\mu_N > 0$. The population size N_t is given by

$$N_t = \varsigma_N z'_t + \mu_N, \quad (15)$$

where z'_t is a random draw from the truncated (maximally asymmetric) Lévy-stable law of exponent $\alpha' \in (1, 2]$ with support $(-\mu_N/\varsigma_N, (R_{t-1} - \mu_N)/\varsigma_N]$. The recruitment R_t is then given by Equation (7). Assume $\varsigma_N/\mu_N \ll 1$. If $R_{t-1} - \mu_N > \varsigma_N$, since the region $|N_t - \mu_N| \gtrsim \varsigma_N$ is typically not sampled, then one typically has $R_t - \mu_N > \varsigma_N$ for a large population with $\langle X \rangle > 1$. So that the

stock-recruitment process is insensitive to the confinement. Consequently, one has $\langle N \rangle \approx \mu_N$, $\langle R \rangle \approx \langle X \rangle \mu_N$, and $\Sigma_N \approx \zeta_N T^{1/\alpha' - 1/2}$ with $T (\gg 1)$ denoting the length of the stochastic process.

By setting $\alpha = \alpha' = 1.42$, and using a population of $\mu_N = 10^5$ to $10^{10.5}$, and three different ζ_N values chosen to give $\zeta_N = \mu_N^{1/2}$, $\mu_N^{1/\alpha}$ and $0.1\mu_N$, I simulated the stock-recruitment process for 10^5 generations for each choice of parameter values, where $\langle X \rangle = \alpha/(\alpha - 1)$ with $x_0 = 1$ in Equation (1).

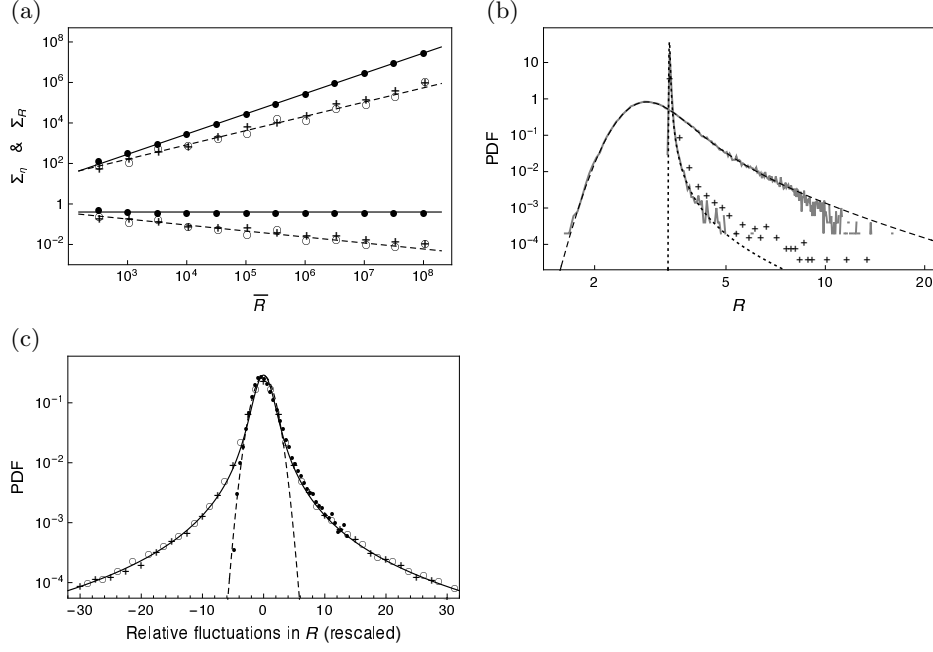


FIG. 2. Lévy-stable model and beyond. Plots are generated by setting $\zeta_N = \mu_N^{1/2}$ (o), $\mu_N^{1/\alpha}$ (+), and $0.1\mu_N$ (●). (a) Fluctuation scaling of R (upper points) and η (lower points). Averages are taken over simulations (R in units of 10^3). (b) Recruitment distributions (plotted on log-log scale, with R in unit of 10^8), generated by setting $\mu_N = 10^8$ and $\langle X \rangle = 3.38$. (c) Rescaled distributions of recruitment growth-rates.

The case of $\zeta_N = \mu_N^{1/2}$ shows in Figure 2a that $\Sigma_R \propto \bar{R}^{1/\alpha}$ (upper open circles with dashed line) with constant prefactor $[\overline{\Sigma_R/\bar{R}^{1/\alpha}}] = 1.26$ (average across simulation sets), and $\Sigma_\eta \propto \bar{R}^{1/\alpha - 1}$ (lower open circles with dashed line) with $[\overline{\Sigma_\eta/\bar{R}^{1/\alpha - 1}}] = 1.39$. The average \bar{R} is calculated from each simulation run. The case of $\zeta_N = \mu_N^{1/\alpha}$ shows in Figure 2a that the Σ_R is still proportional to $\bar{R}^{1/\alpha}$ (upper plus signs), and $\Sigma_\eta \propto \bar{R}^{1/\alpha - 1}$ (lower plus signs). The points for R (resp. η) collapse onto the upper (resp. lower) dashed line. The case of $\zeta_N = 0.1\mu_N$ shows in Figure 2a that $\Sigma_R \propto \bar{R}$ (upper solid circles with solid line) with $[\overline{\Sigma_R/\bar{R}}] = 0.283$, and the Σ_η is independent of \bar{R} (lower solid circles) with $[\overline{\Sigma_\eta}] = 0.357$. The (lower) solid horizontal line is at $\sqrt{2} [\overline{\Sigma_R/\bar{R}}] = 0.400$.

As to the recruitment and growth-rate distributions, Figure 2b and c confirm that as $\langle N \rangle$ gets large, while, when $\Sigma_N / \langle N \rangle^{1/\alpha} \rightarrow 0$, the fluctuations in recruitment and in growth rates are insensitive to external forces, when $\Sigma_N / \langle N \rangle^{1/\alpha} \rightarrow \infty$, the recruitment mimics the population fluctuations except for $R \gtrsim \langle X \rangle (\mu_N + \varsigma_N)$ and for $\eta \gtrsim \sqrt{2} \varsigma_N / \mu_N$.

Figure 2b shows the recruitment distributions for the population of $\mu_N = 10^8$. Equation (8) (dotted line with $\varsigma_N = \mu_N^{1/2}$) and Equation (9) with N_t as in Equation (15) (dashed line with $\varsigma_N = 0.1\mu_N$) agree with the results (noisy gray curves) from the simulations. The dotted line represents the maximally asymmetric Lévy-stable distribution ($\alpha = 1.42$) with mean of $\langle X \rangle \mu_N$ and width of $x_0 C_\alpha \mu_N^{1/\alpha}$. The dashed line represents the maximally asymmetric Lévy-stable distribution ($\alpha = 1.42$) with mean of $\langle X \rangle \mu_N$ and width of $\langle X \rangle \varsigma_N = 0.1 \langle X \rangle \mu_N$.

Figure 2c shows the recruitment growth-rate distributions for the population of $\mu_N = 10^8$. The solid line represents the symmetric Lévy-stable distribution (with exponent $\alpha = 1.42$, mean of zero and width of unity), and the dashed line represents the Gaussian distribution (with mean zero and standard deviation $\sqrt{2}$). For the case $\varsigma_N = \mu_N^{1/2}$ (open circles), the η_t 's are rescaled with $2^{1/\alpha} C_\alpha \mu_N^{1/\alpha - 1} / \langle X \rangle$. For the cases $\varsigma_N = 0.1\mu_N$ (solid circles) and $\varsigma_N = \mu_N^{1/\alpha}$ (plus signs), the η_t 's are rescaled with their root-median-square values.

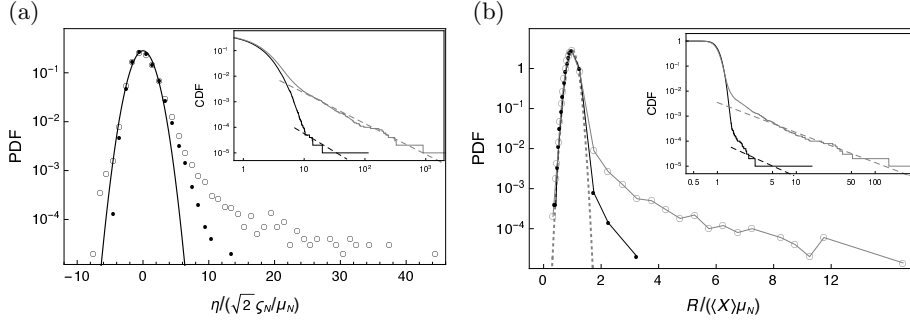


FIG. 3. Aggregate effects of idiosyncratic variations. Plots are generated by setting $\alpha' = 2$ and two different values of $\alpha = 1.42$ (solid circles, and noisy black curves in the insets) and $\alpha = 1.2$ (open circles, and noisy gray curves in the insets), under stochastic variation in population sizes, $\varsigma_N = 0.1\mu_N$ with $\mu_N = 10^8$. (a) Recruitment growth-rate distributions (rescaled with $\sqrt{2}\varsigma_N/\mu_N$). (b) Recruitment distributions with $\langle X \rangle = 6$ (points are binned logarithmically). In the insets, shown are the complementary cumulative distributions.

In the following, I examine how large one can expect aggregate effects of idiosyncratic variations to be. For $\alpha' = 2$, the N_t 's follow the Gaussian distribution centered on μ_N . In this case, shown in Figure 3, one readily sees that recruitment fluctuations in tail part come from idiosyncratic reproductive successes. Using two different values of $\alpha = 1.42$ (solid circles, and noisy black curves in the insets) and $\alpha = 1.2$ (open circles, and noisy gray curves in the insets), under stochastic variation in population sizes, $\varsigma_N = 0.1\mu_N$ with $\mu_N = 10^8$, simulations were run for 10^5 generations for each choice of parameter values, where $\langle X \rangle = 6$. The crossover from

Gaussian to power-law behavior with exponent α occurs at around $\eta = \sqrt{2}\varsigma_N/\mu_N$ for recruitment growth-rate distributions (panel a), and the crossover also occurs at around $R/(\langle X \rangle \mu_N) = 1 + \varsigma_N/\mu_N$ for recruitment distributions (panel b). The black solid line in panel a (resp. the gray dotted line in panel b) represents the Gaussian distribution with mean zero and standard deviation $\sqrt{2}$ (resp. mean one and standard deviation $\sqrt{2}\mu_N/\varsigma_N$). In the insets of Figure 3, where shown are the complementary cumulative distributions, power-laws are seen as straight dashed lines with slopes of -1.42 (black) and -1.2 (gray) on a log-log plot.

6. CONCLUSION

Based on the power-law model of offspring-number distribution with exponent $1 < \alpha < 2$, this paper has provided advances in understanding the empirical properties of recruitment variability in marine fishes. With only minimal ingredients, the Lévy-stable recruitment model is able to capture the aggregate effect of idiosyncratic variations for a large population in a random environment. It establishes a connection between the tail exponents of the distributions at a micro and macro scale, i.e. the offspring-number and recruitment distributions. The value of α may be estimated by examining the DNA sequence variation within a population, and the exponent α characterizes the intermittency properties (rare events of large amplitude) of recruitment (see Niwa et al. 2016, 2017, Niwa 2022b,c).

To what extent individual reproductive outputs are averaged out upon aggregation depends on the magnitude of the year-to-year fluctuations in the number of spawners or the carrying capacity of environment. Even though the fluctuations in population sizes dominate the fluctuations of the sums of individual reproductive outputs, the idiosyncratic reproductive successes can have a noticeable impact on the overall recruitment. One sees the sum-stable (or α -stable) decay in the tails $R_t - \langle R \rangle \gtrsim \Sigma_R$ and $\eta_t \gtrsim \sqrt{2}\Sigma_R/\langle R \rangle$ with $\Sigma_R \propto \langle R \rangle$, as a representation of the idiosyncratic reproductive variability, where the tails follow the power law with the same exponent as the distribution of individual reproductive outputs. When environmental disturbances (such as climate and commercial exploitation) are large enough for the population-size fluctuations to dominate the individual reproductive variations, the symmetry of the Lévy-stable distribution of recruitment growth-rates is broken. One then observes a totally asymmetric distribution with a power-law tail in a large population.

In summary, the linear-scaling behavior $\Sigma_R \propto \langle R \rangle$ (or the independence of Σ_η and $\langle R \rangle$) implies that the individual reproductive variability is dominated by environmentally driven fluctuations in the population size, which leads to asymmetries in the distribution of relative changes in recruitment. The totally asymmetric (skewed to the right) character of the recruitment growth-rate distribution can be a sign of the domination by a single or a few families in the population. The recruitment fluctuations in tail part (i.e. intermittent, strong year-classes) come from idiosyncratic individual-level reproductive successes.

REFERENCES

- Allen, A. P., Li, B. L., & Charnov, E. L. (2001). Population fluctuations, power laws and mixtures of lognormal distributions. *Ecol. Lett.*, 4, 1–3.
- Anderson, R. M., Gordon, D. M., Crawley, M. J., & Hassell, M. P. (1982). Variability in the abundance of animal and plant species. *Nature*, 296, 245–248.

- Árnason, E. & Halldórsdóttir, K. (2015). Nucleotide variation and balancing selection at the *Ckma* gene in Atlantic cod: analysis with multiple merger coalescent models. *PeerJ*, 3, e786.
- Bouchaud, J. P. & Georges, A. (1990). Anomalous diffusion in disordered media: statistical mechanisms, models and physical applications. *Phys. Rep.*, 195, 127–293.
- Carmona, R. & Durrleman, V. (2003). Pricing and hedging spread options. *SIAM Rev.*, 45, 627–685.
- Cobain, M. R. D., Brede, M., & Trueman, C. N. (2019). Taylor’s power law captures the effects of environmental variability on community structure: an example from fishes in the North Sea. *J. Anim. Ecol.*, 88, 290–301.
- Cushing, D. (1990). Plankton production and year-class strength in fish populations: an update of the match/mismatch hypothesis. *Adv. Mar. Biol.*, 26, 249–293.
- Eisler, Z., Bartos, I., & Kertész, J. (2008). Fluctuation scaling in complex systems: Taylor’s law and beyond. *Adv. Phys.*, 57, 89–142.
- Eldon, B., Birkner, M., Blath, J., & Freund, F. (2015). Can the site-frequency spectrum distinguish exponential population growth from multiple-merger coalescents? *Genetics*, 199, 841–856.
- Eldon, B. & Wakeley, J. (2006). Coalescent processes when the distribution of offspring number among individuals is highly skewed. *Genetics*, 172, 2621–2633.
- Gabaix, X. (2011). The granular origins of aggregate fluctuations. *Econometrica*, 79, 733–772.
- Gibrat, R. (1931). *Les Inégalités Économiques*. Paris: Librairie du Recueil Sirey.
- Hedgecock, D. & Pudovkin, A. I. (2011). Sweepstakes reproductive success in highly fecund marine fish and shellfish: a review and commentary. *Bull. Mar. Sci.*, 87, 971–1002.
- Hilborn, R. & Walters, C. J. (1992). *Quantitative Fisheries Stock Assessment: Choice, Dynamics and Uncertainty*. London: Chapman & Hall.
- Hjort, J. (1914). Fluctuations in the great fisheries of the northern Europe viewed in the light of biological research. *Rapp. P.-V. Réun. Cons. Int. Explor. Mer*, 20, 1–228.
- Keitt, T. & Stanley, H. E. (1998). Dynamics of North American breeding bird populations. *Nature*, 393, 257–260.
- Keitt, T. H., Amaral, L. A. N., Buldyrev, S. V., & Stanley, H. E. (2002). Scaling in the growth of geographically subdivided populations: invariant patterns from a continent-wide biological survey. *Phil. Trans. R. Soc. Lond. B*, 357, 627–633.
- Khinchine, A. & Lévy, P. (1936). Sur les lois stables. *C. R. Acad. Sci. Paris*, 202, 374–376.
- Kingman, J. F. C. (1982). The coalescent. *Stoch. Process. Their Appl.*, 13, 235–248.
- Lan, B. L. & Chandran, P. (2011). Distribution of animal population fluctuations. *Physica A*, 390, 1289–1294.
- Lévy, P. (1925). *Calcul des Probabilités*. Paris: Gauthier-Villars.
- Lévy, P. (1937). *Théorie de l’Addition des Variables Aléatoires*. Paris: Gauthier-Villars.
- de Menezes, M. A. & Barabási, A.-L. (2004). Fluctuations in network dynamics. *Phys. Rev. Lett.*, 92, 028701.
- Newman, M. E. J. (2005). Power laws, Pareto distributions and Zipf’s law. *Contemp. Phys.*, 46, 323–351.
- Niwa, H.-S. (2006). Exploitation dynamics of fish stocks. *Ecol. Inform.*, 1, 87–99.
- Niwa, H.-S. (2007). Random-walk dynamics of exploited fish populations. *ICES J. Mar. Sci.*, 64, 496–502.
- Niwa, H.-S. (2022a). Fluctuation scaling in Lévy-stable recruitment of marine fishes in randomly varying environments. *arXiv:2202.06206 [q-bio.PE]*.
- Niwa, H.-S. (2022b). Hatchery-induced transition of the effective size in a Pareto population. *arXiv:2202.07038 [q-bio.PE]*.
- Niwa, H.-S. (2022c). Reciprocal symmetry breaking in Pareto sampling. *arXiv:2202.04865 [math.PR]*.
- Niwa, H.-S., Nashida, K., & Yanagimoto, T. (2016). Reproductive skew in Japanese sardine inferred from DNA sequences. *ICES J. Mar. Sci.*, 73, 2181–2189.
- Niwa, H.-S., Nashida, K., & Yanagimoto, T. (2017). Allelic inflation in depleted fish populations with low recruitment. *ICES J. Mar. Sci.*, 74, 1639–1647.
- Reed, W. J. & Hughes, B. D. (2002). From gene families and genera to incomes and internet file sizes: why power laws are so common in nature. *Phys. Rev. E*, 66, 067103.
- Sargsyan, O. & Wakeley, J. (2008). A coalescent process with simultaneous multiple mergers for approximating the gene genealogies of many marine organisms. *Theor. Popul. Biol.*, 74, 105–114.

- Schweinsberg, J. (2003). Coalescent processes obtained from supercritical Galton-Watson processes. *Stoch. Process. Their Appl.*, 106, 107–139.
- Steinrücken, M., Birkner, M., & Blath, J. (2013). Analysis of DNA sequence variation within marine species using Beta-coalescents. *Theor. Popul. Biol.*, 87, 15–24.
- Takayasu, M., Watanabe, H., & Takayasu, H. (2014). Generalised central limit theorems for growth rate distribution of complex systems. *J. Stat. Phys.*, 155, 47–71.
- Taylor, L. R. (1961). Aggregation, variance and the mean. *Nature*, 189, 732–735.
- Zaliapin, I. V., Kagan, Y. Y., & Schoenberg, F. P. (2005). Approximating the distribution of Pareto sums. *Pure Appl. Geophys.*, 162, 1187–1228.